J. Biochem. **137**, 287–296 (2005)
DOI: 10.1093/jb/mvi031

Dynamic Cytoplasmic Anchoring of the Transcription Factor Bach1 by Intracellular Hyaluronic Acid Binding Protein IHABP

Chikara Yamasaki[1,2], Satoshi Tashiro[1], Yasumasa Nishito[1], Taijiro Sueda[2] and Kazuhiko Igarashi[1,*]

[1]Department of Biomedical Chemistry, Hiroshima University Graduate School of Biomedical Sciences, Kasumi 1-2-3, Hiroshima 734-8551; and [2]Department of Surgery, Hiroshima University Graduate School of Biomedical Sciences, Kasumi 1-2-3, Hiroshima 734-8551

Received November 15, 2004; accepted December 15, 2004

Bach1 functions as a transcriptional repressor of heme oxygenase-1 (HO-1) and the β-globin genes. The enhancer regions of these genes contain multiple Maf recognition elements (MAREs) to which Bach1 can bind. Previous studies have shown that increased levels of heme and cadmium induce the nuclear export of Bach1, resulting in cytoplasmic accumulation. By means of a yeast two hybrid screening using Bach1 as bait, we identified the intracellular hyaluronic acid binding protein (IHABP) as a potential regulator of Bach1. IHABP is a microtubule-associated protein that may regulate the organization of the cytoskeletal network. A series of domain analyses revealed that a region of Bach1 previously implicated in cytoplasmic accumulation was necessary for IHABP-binding. A C-terminal region of IHABP was necessary for Bach1-binding. Overexpressed Bach1 colocalized with IHABP in the cytoplasm, forming fiber-like structures on microtubules. Fluorescence recovery after photobleaching (FRAP) analysis revealed a dynamic nature of the Bach1-IHABP interaction in living cells. The repression of HO-1 reporter activity by Bach1 was attenuated by co-transfecting IHABP in a dose-dependent manner. Moreover, the overexpression of IHABP induced the endogenous HO-1 gene in NIH3T3 cells. The overall results suggest that IHABP regulates the subcelluar localization of Bach1 in order to fine-tune transactivation of Bach1 target genes such as HO-1.

Key words: Bach1, heme, heme oxygenase-1, Maf, oxidative stress.

Abbreviations: Bach1, BTB and CNC homology 1; FRAP, fluorescence recovery after photobleaching; HO-1, heme oxygenase-1; IHABP, intracellular hyaluronic acid binding protein; MARE, Maf recognition element.

Heme oxygenase (HO) regulates the levels of cellular heme and iron by catalyzing the first step of heme degradation, which results in the release of iron, carbon monoxide and the linear tetrapyrrol biliverdin. Biliverdin is subsequently converted to bilirubin by the enzyme biliverdin reductase (*1*, *2*). Recently, HO-1, one of the HO isozymes, has been widely recognized as a ubiquitous and important protective enzyme in response to various conditions of cellular stress. While HO-1 protects cells by removing the pro-oxidant heme and generating catalytic products with antioxidant, anti-inflammatory activities, the cytoprotective function of HO-1 is manifested only after its induction in response to diverse insults such as heme, UV light, heavy metals, glutathione depletion, and H_2O_2 (*3*–*7*).

The enhancer regions of the HO-1 gene (*hmox-1*) contain multiple Maf recognition elements (MAREs) that mediate inducible expression (*8*, *9*). The small Maf proteins (MafF, -G, and -K) are dual-function transcription factors that repress or activate *hmox-1* depending on their heterodimer partners. The small Maf/Bach1 heterodimers bind to the *hmox-1* MAREs to repress its expression. The exchange of the small Maf dimerization partner from Bach1 to Nrf2 is a key event in the switch from repression to activation of *hmox-1* (*10*–*15*). Both heme and cadmium, strong inducers of *hmox-1*, promote the switching of heterodimers on the *hmox-1* enhancers in cells. While Bach1 localizes in the nucleus under normal conditions when expressed together with small Maf proteins, it is exported from the nucleus to the cytoplasm in a Crm1 dependent manner in response to cadmium and heme (*16*, *17*). Bach1 carries two separate nuclear export signals, each mediating specific responses to heme or cadmium. Whereas the C-terminal region, termed the cytoplasmic localization signal (CLS), mediates cadmium-activated nuclear export, another region containing three heme-binding motifs functions as a heme-activated nuclear export signal [(*16*, *17*), see Fig. 1A]. These observations indicate that the regulation of the subcellular localization of Bach1 is critical for the fine-tuning of *hmox-1* expression. In addition to these two nuclear export signals, we found a region of Bach1 that facilitates cytoplasmic accumulation (see Fig. 1). Because this region is not a nuclear export signal, it may bind to a cytoplasmic protein to anchor Bach1 (*16*). To search for a protein that realizes such a regulation, we carried out yeast two hybrid screening using Bach1 as bait. We report here that intracellular hyaluronic acid binding protein (IHABP), also known as the receptor for hyaluronan-mediated motility (RHAMM) (*18*–*22*), is a potential

*To whom correspondence should be addressed. Fax: +81-82-257-5139, E-mail: igarak@hiroshima-u.ac.jp

regulator of Bach1, and, hence, the expression of *hmox-1*. We show that IHABP mediates the anchoring of Bach1 to the cytoskeleton, causing the induction of HO-1. Fluorescence recovery after photobleaching (FRAP) experiments revealed the dynamic interaction of Bach1 and IHABP in a living cell. Our results suggest that in addition to heme and cadmium, Bach1 may receive signals from cytoskeletal structures to regulate *hmox-1* expression.

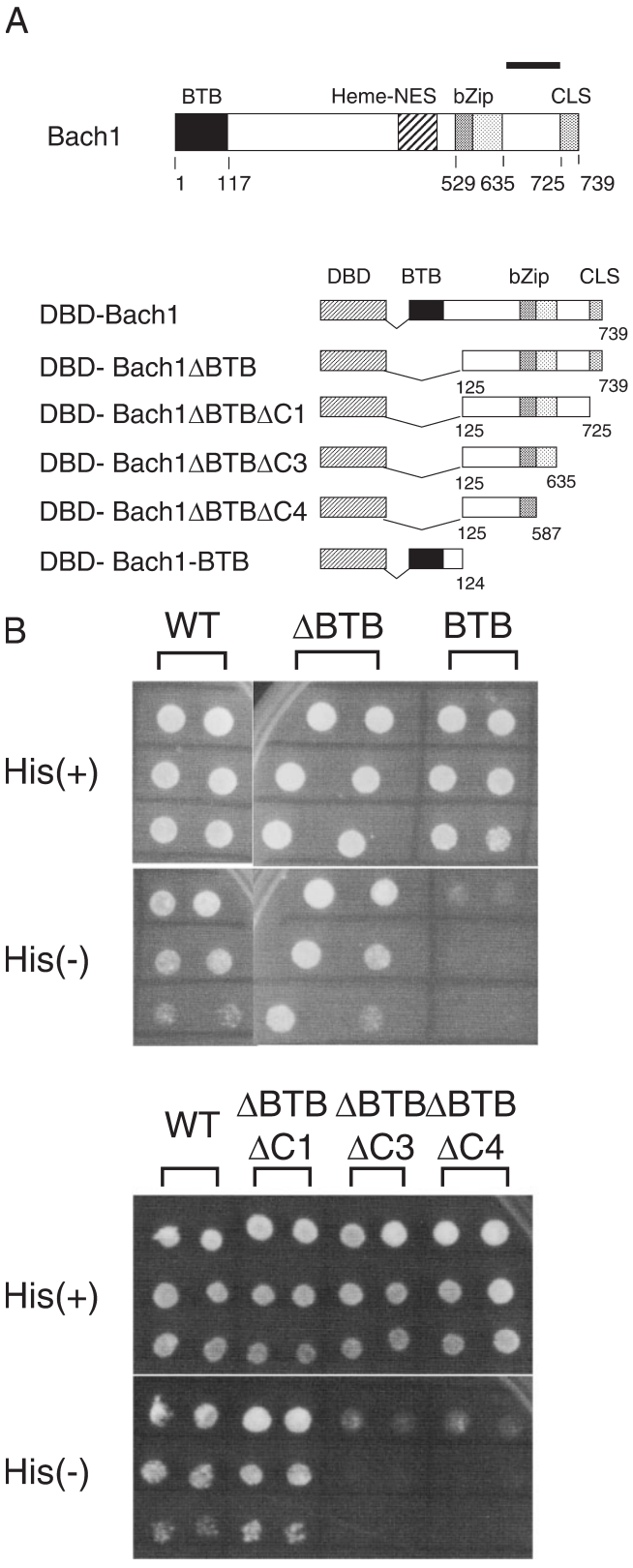

Fig. 1. **Mapping of the IHABP-binding region on Bach1 in yeast two hybrid assays.** (A) Schematic representations of Bach1 and its deletion derivatives fused with the GAL4 DBD are shown. The thick line above Bach1 indicates the putative cytoplasmic anchoring region defined in our previous study (*16*). (B) Bach1 deletion derivatives were examined for binding to IHABP in yeast two hybrid assays. Growth on selection plates lacking histidine suggests a positive interaction. DBD-Bach1ΔBTB and DBD-ΔBTBΔC1 supported proliferation in the absence of histidine only when co-expressed with AD-IHABP.

MATERIALS AND METHODS

Reagents—Restriction endonucleases and other DNA-modifying enzymes were purchased from either New England Biolabs or Takara. Oligonucleotides were synthesized by Invitrogen. Reagents for luciferase assays were purchased from Promega. All other chemicals were reagent grade.

Cell Culture—HEK293T cells and NIH3T3 cells were cultured in Dulbecco's modified Eagle's medium (Sigma) with 10% fetal bovine serum (JRH BioSciensces), 100 units/ml penicillin and 100 μg/ml streptomycin (Invitrogen).

Plasmids—The bait plasmid for two hybrid screening was constructed by inserting the *Sal*I fragment of mouse Bach1 cDNA (*23*) into the *Bam*HI site of pGBT9 (Clontech) after filling in the relevant DNA ends. The resulting plasmid, pGBT-Bach1, encoded the entire Bach1 ORF fused with the DNA binding domain (DBD) of GAL4. The pGBT-Bach1 plasmid was digested with *Eco*RI, and then self-ligated to yield pGBT-Bach1ΔBTB. pGBT-Bach1 was digested with *Bgl*II and *Sal*I, and then self-ligated to yield pGBT-Bach1-BTB. PGBT-Bach1ΔBTBΔC1, pGBT-Bach1ΔBTBΔC3 and pGBT-Bach1ΔBTBΔC4 were constructed by inserting *Eco*RI–*Sal*I fragments from Bach1ΔC1, Bach1ΔC3 and Bach1ΔC4 cDNAs (*14*, *16*, *17*, *23*) into *Eco*RI and *Sal*I-digested pGBT9. Mammalian expression plasmids for FLAG-tagged Bach1, Bach1ΔBTB, Bach1ΔC1, ΔC3, and ΔC4 were described previously (*16*, *17*). pEGFP-IHABP, encoding a fusion of EGFP and the entire type A IHABP, was described previously (*19*, *20*). pGFP-IHABP was digested with *Sac*I and inserted into the *Sac*I site of the pEGFP-C2 vector, resulting in pEGFP-IHABP(1-502). pEGFP-IHABP was digested with *Sac*I and *Hpa*I, and inserted into the *Sac*I–*Sma*I sites of pEGFP-C2 vector, resulting in pEGFP-IHABP(1-464). pEGFP-IHABP was digested with *Sma*I and *Sal*I and inserted into the *Bam*HI site of the pcDNA3.1B FLAG vector by blunt-end ligation, resulting in pcDNA3.1BFLAG-IHABP. The N-terminal portion of IHABP was PCR amplified with primers HR-37F-B (5′-GTTAAGAATGATCAATGTCCTTTCCTAAGGCGCCC-3′) and HR-1428R-B (5′-GTTAAGAATGATCATTACGCTTTATAGCTTTCAAATTG-3′), digested with *Bcl*I, and inserted into the *Bam*HI site of the pcDNA3.1BFLAG vector, resulting in pcDNA3.1BFLAG-IHABP(1-464). pcDNA3.1BFLAG-IHABP was digested with *Hin*dIII and self-ligated to yield pcDNA3.1BFLAG-IHABP(1-166). pcDNA3.1BFLAG-

IHABP was digested with *Hpa*I and *Hin*dIII, and the resulting fragment was inserted into the *Bam*HI (blunted) and *Hin*dIII sites of the pcDNA3.1BFLAG vector, resulting in pcDNA3.1BFLAG-IHABP(465-724). The HO-1 reporter plasmid was described previously (*12*, *14*) and a kind gift of Dr. J. Alam.

Yeast Two-Hybrid Screening—Two-hybrid screening in *Saccharomyces cerevisiae* was performed using the Matchmaker two-hybrid system (Clontech) as described previously (*23*). A mouse day 17 post coitus embryonic Matchmaker cDNA library (Clontech) was transformed into the HF7c yeast strain along with the Bach1 bait plasmid, and selected for colony formation in the absence of histidine. To confirm protein interactions in yeast cells, HF7c cells were transformed with various combinations of plasmids that express DBD-tagged and activation domain (AD)-tagged molecules. Transformants were serially diluted in water and spotted onto His^- and His^+ media to test for the activation of the GAL4-dependent *HIS3* reporter gene.

Immunocytochemistry—HEK293T cells were transfected with various FLAG-tagged Bach1 expression plasmids and/or various GFP-tagged IHABP expression plasmids, and cultured for 24 h. The cells were fixed with 4% paraformaldehyde in phosphate-buffered saline (PBS) for 10 min at room temperature. After fixing, the cells were washed in PBS and permeabilized in 0.5% Triton X-100 in PBS for 5 min. Cells were washed and treated for 30 min at 37°C with the anti-FLAG antibody (Sigma) at a dilution of 1:500–1:1,000. Cells were washed three times in PBS and then treated with fluorescein-conjugated anti–mouse IgG antibodies diluted in 1% bovine serum albumin/ PBS at a concentration of 1:200 at 37°C for 30 min. After washing, the cells were counter-stained with 10 μM Hoechst 33342 and mounted in Vectashield (Vector). The cells were then examined by fluorescence microscopy. NIH3T3 cells were transfected with expression plasmids for FLAG-tagged IHABP, IHABP(1-464), Bach1, or MafK and cultured for 36 h. The cells were fixed and stained with anti-FLAG (mouse) and anti–HO-1 (rabbit) antibodies as described above. Cells were then treated with Cy3-conjugated sheep anti–mouse IgG antibodies and FITC-conjugated goat anti–rabbit antibodies.

Coimmunoprecipitation—HEK 293T cells in 10-cm-diameter dishes were transfected with FLAG-tagged plasmids and other plasmids for 36 h. The cells were washed twice with ice cold 4% PBS and were lysed in buffer C [20 mM HEPES pH 7.9, 20% glycerol, 400 mM NaCl, 1 mM EDTA, 1 mM $MgCl_2$, 0.5 mM DTT, 0.5 mM PMSF, 0.1% NP-40, 1× protease inhibitor cocktail (Roche)]. The whole-cell extracts were pre-cleared by centrifugation and a three-times volume of ID(O) buffer (20 mM HEPES, 20% glycerol, 5 mM $MgCl_2$, 1 mM DTT, 1.3 mg/ml BSA, 1× protease inhibitor cocktail) was added. Extracts were incubated with anti–FLAG M2 affinity gel (Sigma). Immunoprecipitates were washed four times with the wash buffer (10 mM Tris-HCl pH 7.5, 100 mM NaCl, 2 mM EDTA, 0.01% NP-40). The immunoprecipitates were separated by SDS–polyacrylamide gel electrophoresis (PAGE, 7.5% gels unless indicated otherwise). Following SDS-PAGE, the proteins were electro-transferred to PVDF membrane (Millipore). The membranes were blocked for 1 h at 25°C in blocking buffer (3% skimmed milk, 0.05% Tween 20 in TBS), and subsequently incubated with primary and secondary antibodies in the blocking buffer for 1 hour at 25°C. To detect immunoreactive proteins, we used ECL blotting reagents (Amersham).

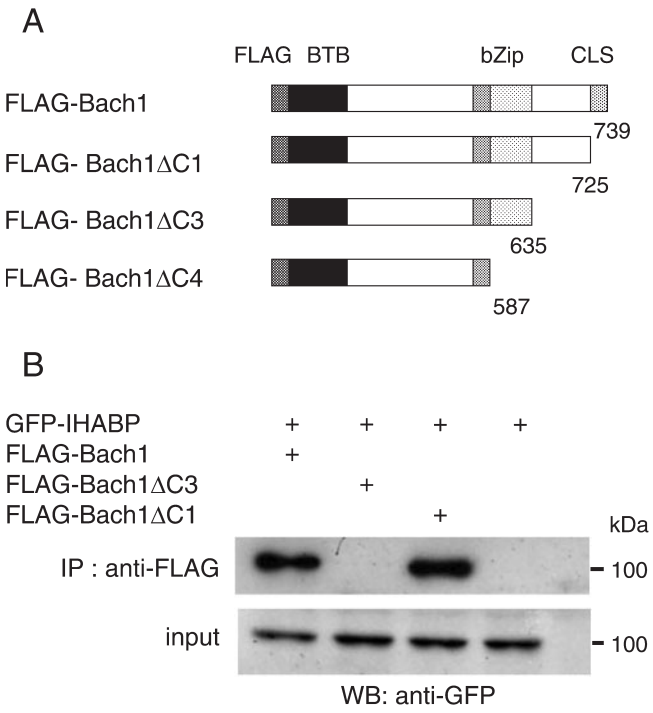

Fig. 2. **Mapping of the IHABP-binding region on Bach1 in mammalian cells.** (A) Schematic representations of Bach1 deletion derivatives tagged with the FLAG epitope are shown. (B) 293T cells were transfected with the indicated combinations of expression plasmids. Cell extracts were immunoprecipitated with FLAG antibody and analyzed by immunoblotting using GFP antibody. Inputs are shown below.

Photobleaching Experiments—Fluorescence recovery after photobleaching (FRAP) was performed with a Zeiss LSM510 confocal laser scanning microscope with a 63×/1.4 plan-apochromat objective (*24*). Cells on round coverslips were transferred to a live-cell chamber FCS2 (Bioptecs), mounted on the microscope stage, and kept at 37°C. The objective was operated with an objective heater as part of the FCS2 system. The fluorescence recovery of HcRed-Bach1 and EGFP-IHABP, bleached with a 543-nm HeNe-laser (0.5 mW) and a 488-nm argon laser at 100% power, respectively, was monitored at 1% power at time intervals as indicated in Fig. 5. Relative intensities in the bleached area were measured and normalized to the average intensity before bleaching.

Reporter Assays—HEK 293T cells were transfected with the reporter plasmid together with various combinations of expression plasmids for Bach1 and IHABP using FuGene6 (Roche). Cells were cultured for 24 h and cell lysates were prepared using the Luciferase Assay System (Promega) following the supplier's protocol. Luciferase activities were measured with a Biolumat Luminometer (Berthold). Firefly luciferase activity was normalized to transfection efficiency as determined from the control sea pansy luciferase activity (*25*). Three inde-

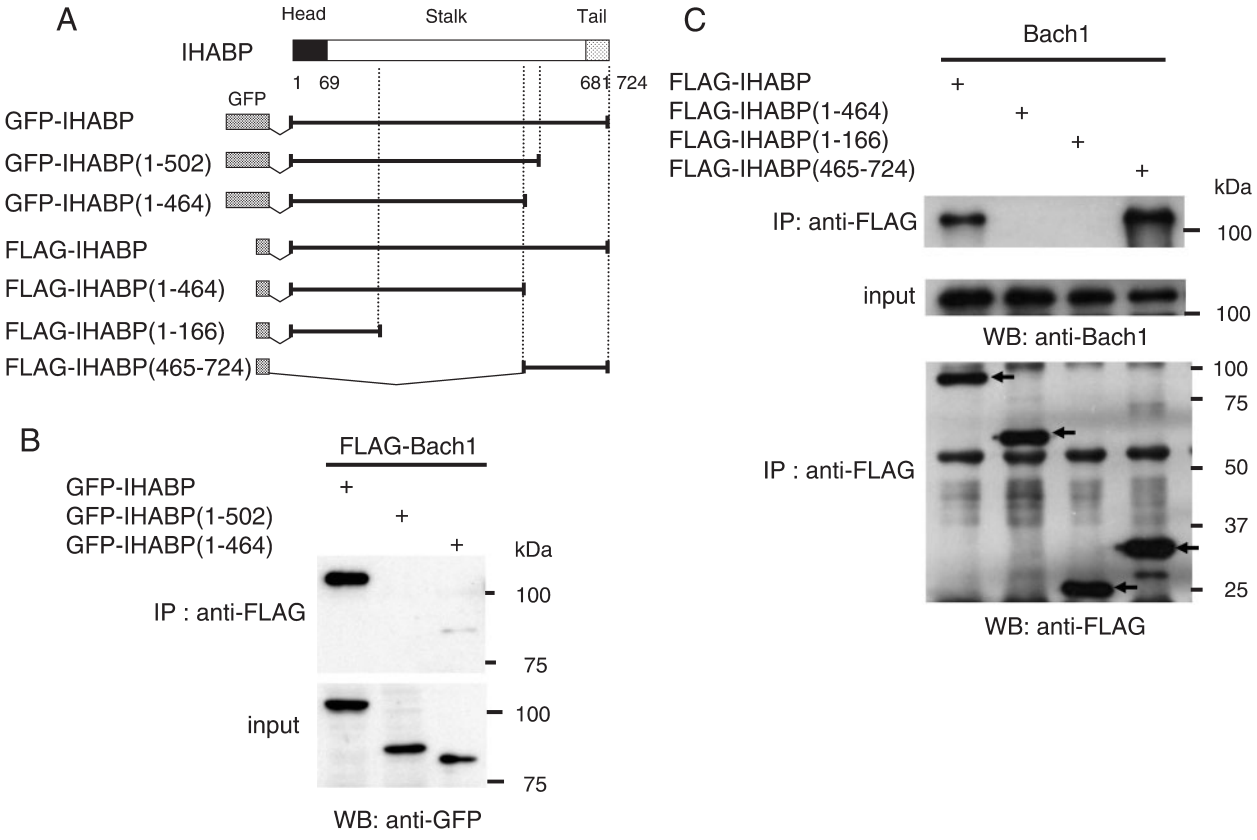

Fig. 3. **Mapping of the Bach1-binding site on IHABP in mammalian cells.** (A) Schematic representations of IHABP and its deletion derivatives tagged with EGFP or FLAG are shown. Three structural domains of IHABP are also shown: the amino-terminal head (amino acid residues 1–69), which interacts with microtubules; an extensive coil coiled stalk (aa 70–680); and a short carboxy-terminal tail (aa 681–724) (*20*). (B) 293T cells were transfected with expression plasmids for FLAG-Bach1 and the indicated EGFP-IHABP. Immunoprecipitation and immunoblotting were carried out using the indicated antibodies. (C) 293T cells were transfected with expression plasmids for Bach1 and the indicated FLAG-tagged IHABP fragments. Immunoprecipitation and immunoblotting were carried out using the indicated antibodies. Expression and immunoprecipitation of IHABP fragments was confirmed by immunoblotting using an anti-FLAG antibody (lower panel; bands are shown with arrows).

pendent experiments, each carried out in duplicate, were performed, and the results were averaged and diagrammed with the standard errors.

RESULTS

Isolation of IHABP as a Bach1-Binding Pprotein—Yeast two hybrid screening was used to identify proteins that bind to Bach1. The bait plasmid expressed the full-length mouse Bach1 fused to the DNA binding domain of GAL4. Most of the candidate clones isolated from the mouse day 17 embryo cDNA library were found to encode small Maf proteins (MafF, -G, or -K) or Bach1. Small Maf proteins are the authentic dimerization partners of Bach1 through leucine zipper interaction, whereas Bach1 forms homo-oligomer through BTB domain–mediated interaction. Isolation of these cDNAs verified the specificity of selection. In addition to small Maf and Bach1, several clones were found to encode a C-terminal portion of IHABP.

Mapping of an IHABP-Binding Site on Bach1—Our aim was to identify a protein that binds to Bach1 through the putative cytoplasmic anchoring domain. We first tried to map an IHABP-binding site on Bach1. Bach1 deletion derivatives truncated at the N- or C-terminus (Fig. 1A) were examined for binding to IHABP in yeast two hybrid assays (Fig. 1B). DBD-Bach1, DBD-Bach1ΔBTB, and DBD-Bach1ΔBTBΔC1 supported proliferation without histidine in the presence of the activation domain (AD)-tagged IHABP (Fig. 1B and data not shown). In contrast, DBD-Bach1-BTB, DBD-Bach1ΔBTBΔC3, DBD-Bach1-ΔBTBΔC4 did not support proliferation without histidine. These results indicate that the region of Bach1 between bZip and CLS is necessary for binding to IHABP. Next, we confirmed the binding of IHABP and Bach1 in mammalian cells by employing co-immunoprecipitation experiments using various fragments of Bach1 (Fig. 2A). Consistent with the results of the yeast two hybrid assays, Bach1 and Bach1ΔC1 co-immunoprecipitated with IHABP in HEK293T cells (Fig. 2B). In contrast, Bach1-ΔC3 did not co-immunoprecipitate. These results confirm that the region between bZip and CLS of Bach1 is required for IHABP-binding. This region overlaps with the putative cytoplasmic anchoring region defined in our previous study [(*16*), see Fig. 1A].

Mapping of a Bach1-Binding Site on IHABP—To map a Bach1-binding site on IHABP, we constructed GFP-tagged IHABP deletion derivatives (Fig. 3A) and carried

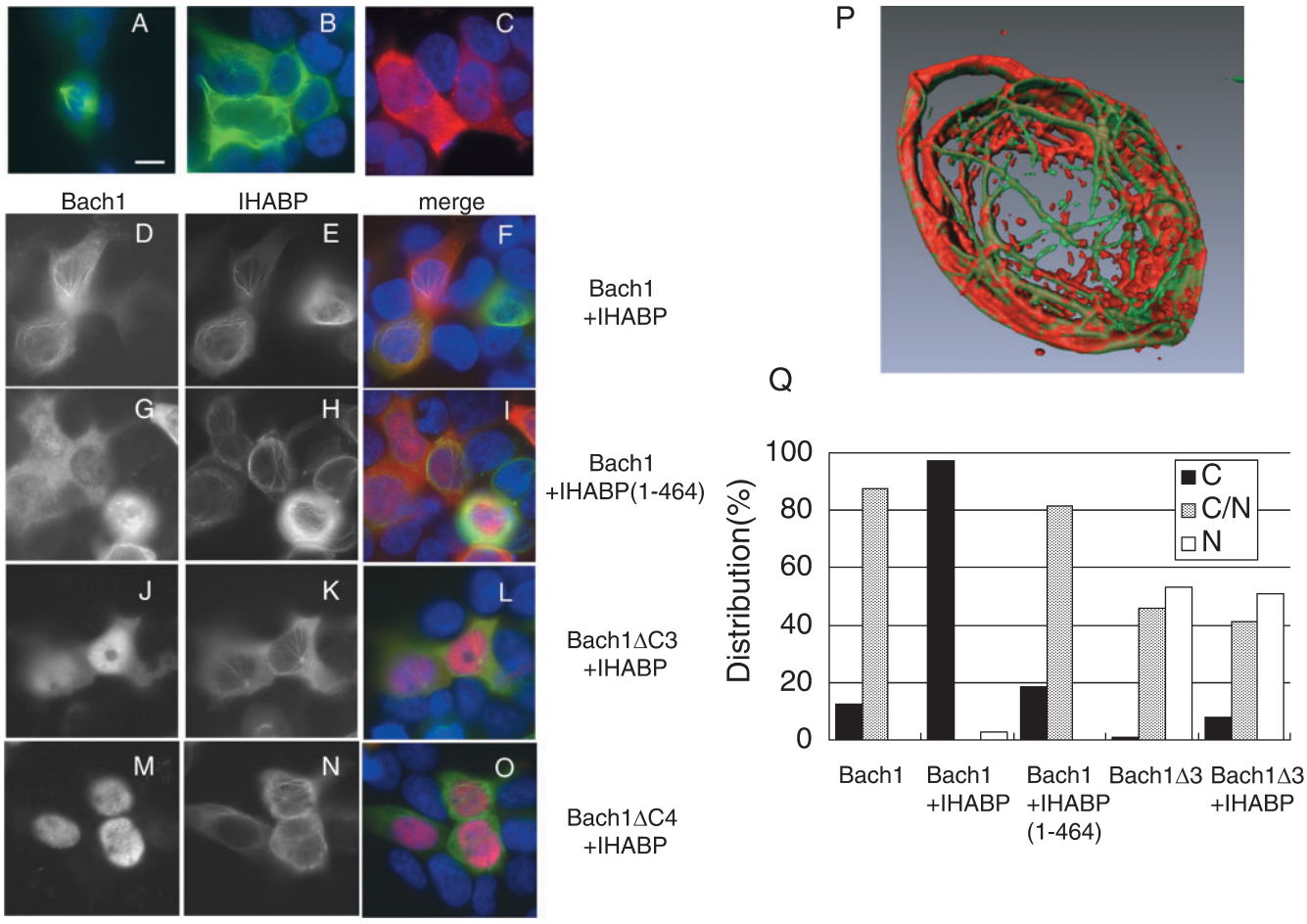

Fig. 4. **Specific colocalization of Bach1 with IHABP.** 293T cells were transfected with expression plasmids for various FLAG-tagged Bach1 and/or EGFP-tagged IHABP derivatives. Proteins were visualized by confocal microscopy with anti-FLAG antibodies and EGFP fluorescence. (A and B) EGFP-IHABP was expressed alone. Cells in M phase (A) and interphase (B) are shown. (C) FLAG-Bach1 was expressed alone. (D–F) FLAG-Bach1 and EGFP-IHABP were co-expressed. Bach1 (D), IHABP (E), and merged image (F). (G–I) FLAG-Bach1 and EGFP-IHABP(1-464) were co-expressed. Bach1 (G), IHABP (H), and merged image (I). (J–O) FLAG-Bach1ΔC3 or ΔC4 and EGFP-IHABP were co-expressed. Bach1 (J and M), IHABP (K and N), and merged images (L and O). (P) 3D reconstruction from light optical sections of 293T cells expressing EGFP-IHABP (green) and FLAG-Bach1 (red). (Q) 293T cells were transfected with the indicated expression plasmids. The subcellular localization of Bach1 was classified into three categories: C, cytoplasmic-dominant accumulation (black bar); C/N, roughly equal distribution in cytoplasmic and nuclear compartments (grey bar); and N, nuclear-dominant accumulation (white bar). Results of counting 200 cells are shown.

out co-immunoprecipitation experiments in HEK 293T cells. GFP-IHABP co-immunoprecipitated with Bach1, confirming a specific interaction (Fig. 3B). In contrast, GFP-IHABP(1-464) and GFP-IHABP(1-502) did not co-precipitate with Bach1. Thus, the Bach1-binding site on IHABP maps within its C-terminal region. This is consistent with the fact that the C-terminal region of IHABP was isolated in the initial two hybrid screening. To confirm that the C-terminal region of IHABP is sufficient for binding to Bach1, we constructed the additional FLAG-tagged deletion derivatives IHABP(1-464), IHABP(465-724) and IHABP(1-166) (Fig. 3A). When co-expressed with Bach1, only IHABP(465-724) co-precipitated Bach1 (Fig. 3C). In conclusion, the Bach1-binding site on IHABP maps in the C-terminal region of IHABP between residues 503 and 724.

Bach1 Colocalizes with IHABP—IHABP possesses a microtubule-binding region in the extreme N terminus (see Fig. 3A) that mediates interactions with microtubules and actin filaments *in vitro* and *in vivo* (*20*). This fact prompted us to examine whether IHABP affects the subcellular localization of Bach1. IHABP accumulated within the cytoplasm when expressed in HEK 293T cells. Consistent with previous reports (*18*, *20*), we often observed that IHABP formed fiber-like structures (Fig. 4, A and B). When Bach1 was expressed in HEK 293T cells, it distributed diffusely in both the nucleus and cytoplasm, with intense staining in the cytoplasm (Fig. 4C). When Bach1 was co-expressed with IHABP, Bach1 was excluded from the nuclear region (Fig. 4, D–F and Q). Furthermore, when IHABP formed fiber-like structures, Bach1 co-localized with the IHABP fibers (Fig. 4, D–F). Three-dimensional analysis of Bach1-IHABP distribution clearly indicated their close association on fiber-like structures (Fig. 4P). These results suggest that IHABP

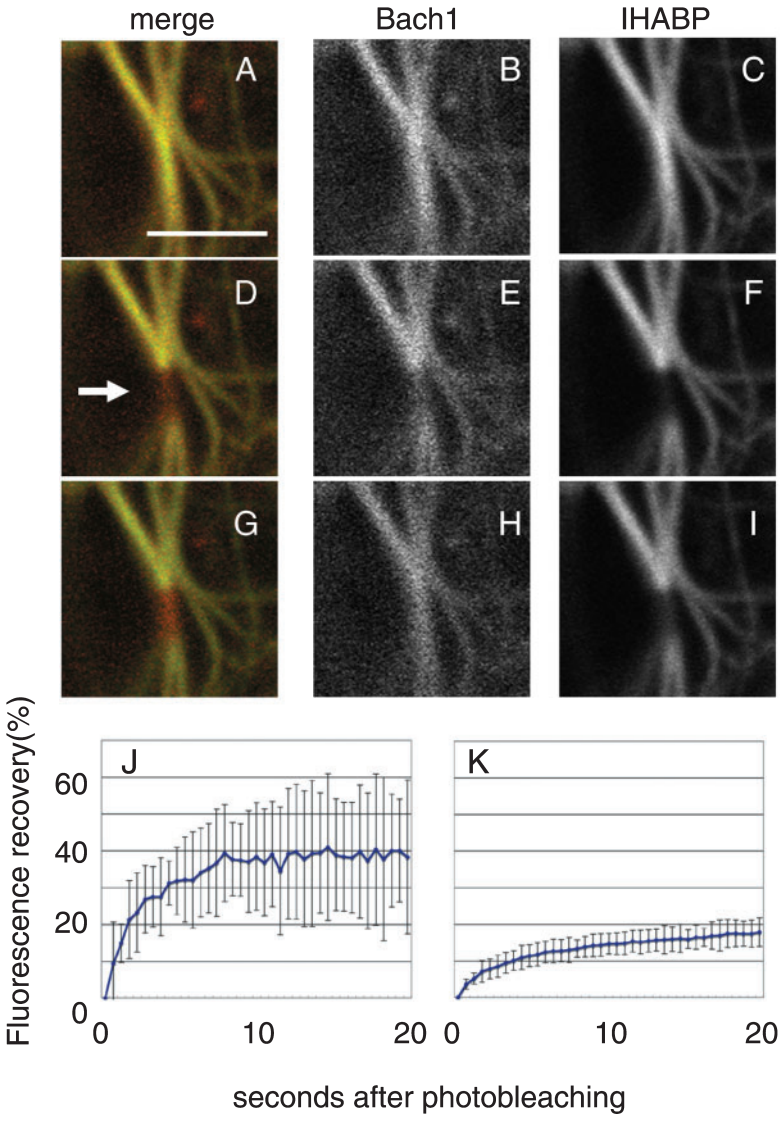

Fig. 5. **Dynamic interaction of Bach1 and IHABP.** Cells expressing HcRed-Bach1 and EGFP-IHABP were subjected to a local bleach pulse, and the kinetics of fluorescence recovery in the bleached area was determined. (A–I) An example of the primary data obtained using the photobleaching protocol. The arrow indicates a photobleached area. Merged images of HcRed-Bach1 and EGFP-IHABP (A, D, G), HcRed-Bach1 (B, E, H) or EGFP-IHABP (C, F, I) before photobleaching (A–C), just after photobleaching (D–F), and 20 s after photobleaching (G–I) are shown. Bar, 5 μm. (J and K) Quantitative FRAP analysis of HcRed-Bach1 (J) and EGFP-IHABP (K). Recovery of fluorescence was measured at the indicated time points after the bleach pulse. All data points represent the means of 5 different measurements, and the error bars indicate twice the standard error. Intensities before and just after photobleaching were set to 100 and 0%, respectively.

may play a role in Bach1 anchoring on microtubule-containing structures within the cytoplasm.

To examine the correlation between Bach1-IHABP binding and the observed co-localization, we compared the subcellular localizations of truncated forms of Bach1 and IHABP lacking respective binding regions (Fig. 4, G–O). IHABP(1-464) formed the same fiber-like structures on microtubules as the full-length IHABP (Fig. 4H). This is consistent with the presence of the microtubule-binding region on IHABP(1-464) (Fig. 3A). Co-expressed Bach1 localized diffusely in both the nucleus and the cytoplasm without showing any fiber-like structures on microtubules (Fig. 4G). Next, we co-expressed Bach1Δ3 (Fig. 4, J–L) or Bach1Δ4 (Fig. 4, M–O) together with the full-length IHABP in HEK 293T cells. While Bach1Δ3 was observed in both nuclear and cytoplasmic regions, Bach1Δ4 was found predominantly in the nucleus (Fig. 4, J, M, Q, and data not shown). Importantly, these fragments did not show co-localization with IHABP in the cytoplasm (Fig. 4, L and O). These results suggest that IHABP anchors Bach1 on microtubules in the cytoplasm through a direct interaction with Bach1.

Dynamic Interaction of Bach1 and IHABP—As described above, immunofluorescence staining revealed that Bach1 and IHABP colocalize on microtubules. Such a structure may irreversibly inactivate Bach1 by achieving static anchoring. Alternatively, the Bach1-IHABP interaction may be dynamic, allowing a conditional regulation. To distinguish these possibilities, we investigated the dynamics of Bach1 and IHABP on microtubules in living cells by performing fluorescence recovery after photobleaching (FRAP) analysis (*24*, *26*). A HcRed-Bach1 expression plasmid was co-transfected with a GFP-IHABP expression plasmid into GM02063 cells 24 h before FRAP analysis. After simultaneous photobleaching of the HcRed and GFP signals on microtubules (Fig. 5, D–F), the fluorescence recovery of each signal in the bleached region was measured (Fig. 5, G–I). Interestingly, the recovery patterns of the fluorescence signals were different between Bach1 and IHABP. HcRed-Bach1 showed very rapid recovery that was complete within ~10s after bleaching. On the other hand, GFP-IHABP showed relatively slow fluorescence recovery. Quantitative data sets are shown in Fig. 5, J and K. These results

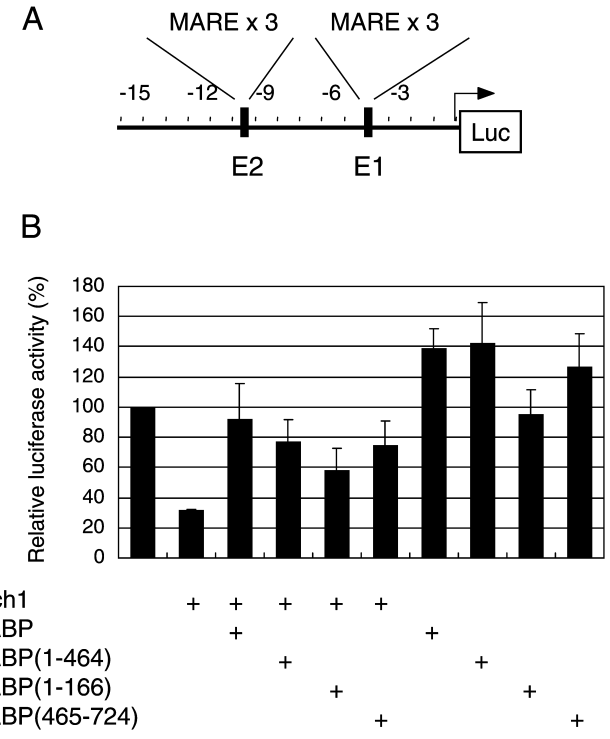

Fig. 6. **IHABP attenuates Bach1-mediated repression of the HO-1 gene reporter.** (A) Schematic representations of the HO-1 reporter. The HO-1 reporter contains several MARE sequences within the enhancer regions that are bound by Bach1. (B) 293T cells were cotransfected with the HO-1 reporter with or without FLAG-Bach1, FLAG-IHABP, FLAG-IHABP(1-464), FLAG-IHABP(1-166), and FLAG-IHABP(465-724). The experiments were performed in triplicate, and the luciferase activities were normalized to *Renilla* luciferase activity.

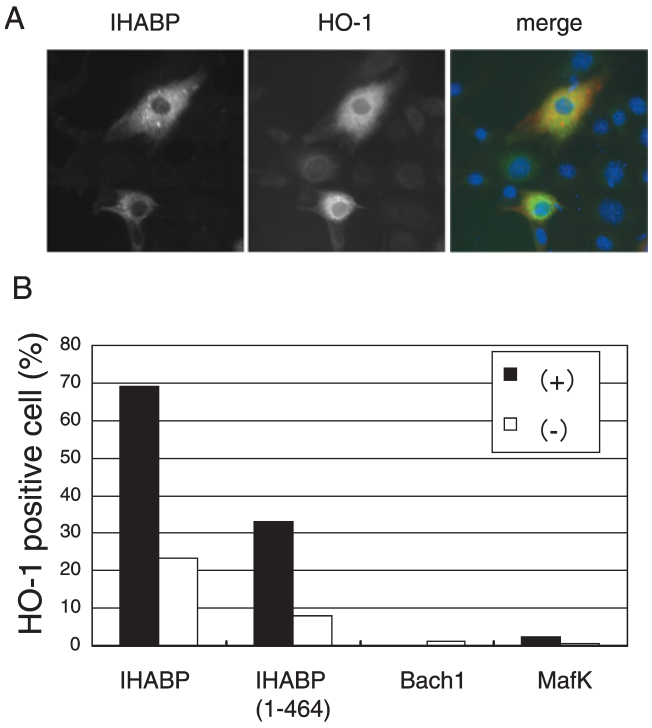

Fig. 7. **IHABP induces the expression of endogenous HO-1 gene.** (A) NIH3T3 cells proliferating on glass coverslips were transfected with expression plasmids for FLAG-IHABP. After 36 h, the cells were stained for IHABP and HO-1. The merged image shows IHABP (red), HO-1 (green), and nuclei (blue). (B) NIH3T3 cells were transfected with expression plasmids for FLAG-IHABP, FLAG-IHABP(1-464), FLAG-Bach1, or FLAG-MafK. The frequencies of HO-1 expressing cells were counted in both FLAG-positive cells (+) and apparently FLAG-negative cells (–) on the same coverslips.

indicate that Bach1 and IHABP have different binding properties to microtubules: while IHABP forms a static structure, Bach1 is in dynamic equilibrium.

IHABP Attenuates the Repression of HO-1 by Bach1—Considering that the HO-1 gene is repressed by Bach1, we next investigated whether IHABP might influence HO-1 gene repression by Bach1. We examined the influence of IHABP on HO-1 reporter activity in transfection assays. The HO-1 reporter contains several MARE sequences within the enhancer regions that are bound by Bach1 (Fig. 6A). As shown previously (*14*), the HO-1 reporter activity was repressed by Bach1. When IHABP was co-expressed, the Bach1-mediated repression was attenuated by IHABP in a dose-dependent manner (Fig. 6B and data not shown). IHABP(465-724) also attenuated the repression by Bach1 (Fig. 6B), consistent with its ability to bind to Bach1. Unexpectedly, IHABP(1-464) and IHABP(1-166) that lacked the Bach1-binding site also attenuated the repression by Bach1 (Fig. 6B). Although the molecular basis for this effect is not clear, these IHABP fragments may cause this effect through their binding to microtubules, which then transmit a signal to activate MARE-dependent gene expression. One possibility is that in addition to its inhibitory effect upon Bach1, IHABP may activate transcription factors such as Nrf2, counteracting the repressor activity of Bach1. Consistent with this idea, both IHABP(1-464) and the wild-type IHABP showed weak activation of the HO-1 reporter activity in the absence of Bach1 (Fig. 6B). However, IHABP(1-166) did not affect the basal reporter activity. Further analysis is required to understand the molecular basis underlying the observed effects.

Having shown that IHABP modulate HO-1 reporter activity, we next investigated whether the overexpression of IHABP induces the expression of the endogenous HO-1 gene. We showed previously that the HO-1 gene is repressed by Bach1 in NIH3T3 cells under normal culture conditions, and that the departure of Bach1 from the enhancers precedes gene expression (*14*, *15*). Using this system, we examined whether IHABP regulates the HO-1 gene. We overexpressed IHABP in NIH 3T3 cells and examined the expression of endogenous HO-1 by immunofluorescent staining (Fig. 7A). More than 60% of the IHABP-expressing cells detected by FLAG staining expressed endogenous HO-1 at high levels. When IHABP non-expressing cells were examined, most of these cells were negative for HO-1 staining, and only 20% expressed HO-1 (Fig. 7, A and B). It should be noted that some of these cells judged to be IHABP-non expressing may actually express IHABP since the HO-1-expression frequency was below 10% in mock-transfected cells. Importantly, deletion of the C-terminal region of IHABP significantly reduced the effect on HO-1 expression (Fig. 7B). However,

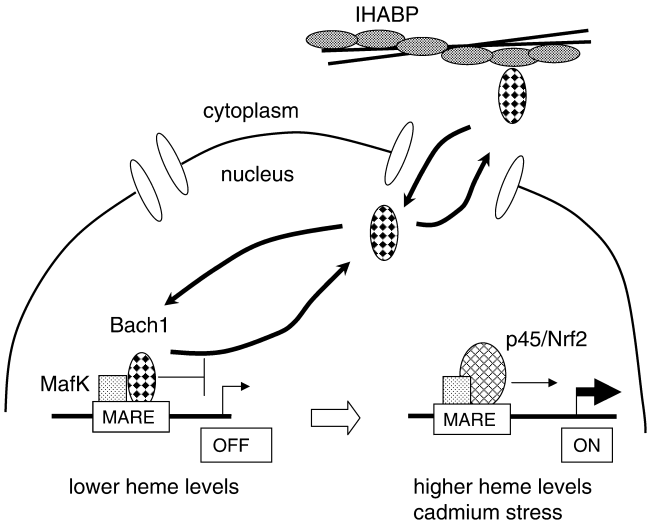

Fig. 8. **A model describing the regulation of ho-1 or other target genes by Bach1 and IHABP.** In addition to MafK, other Maf-related factors may also serve as partners for Bach1. Bach1 occupies MARE enhancers to repress transcription under normal conditions. An increase in heme or cadmium levels alleviates Bach1-mediated repression through the inhibition of its DNA binding activity, nuclear export, and subsequent dynamic trapping by the cytoplasmic IHABP, making MAREs available for activating Maf complexes including Nrf2 or p45 NF-E2.

the effect on HO-1 induction was not completely lost by deleting the C-terminal Bach1 binding domain. This observation again suggests a Bach1-independent activity of IHABP upon gene expression that may be related to the observations in the reporter gene assays described in Fig. 6B. The induction of endogenous HO-1 by IHABP was judged to be specific because neither Bach1 nor MafK expression produced this effect (Fig. 7B). We consider that these results are consistent with the interpretation that IHABP anchors Bach1 on microtubules in cytoplasm to counteract HO-1 repression by Bach1.

DISCUSSION

Based on its interaction with cytoskeletal proteins, IHABP has been suggested to play a role in the organization of the cytoskeletal network, and thus cell morphology and motility (*27*). In PC12 cells, IHABP interacts with extracellular regulated kinase (ERK), suggesting an additional role for IHABP in signal transduction (*28*). In this study, we identified IHABP as a potential regulator of Bach1. The identification of an IHABP-Bach1 interaction suggests that IHABP regulates gene expression by sequestering Bach1 in the cytoplasm. Several lines of evidence support this notion. First, we confirmed the interaction in both yeast and mammalian cells. Second, the IHABP-binding region of Bach1 overlaps with the region that is important for the cytoplasmic accumulation of Bach1 (*16*). Consistently, the subcellular localization of Bach1ΔC3 and Bach1ΔC4 lacking the interacting region was not affected by IHABP. A direct interpretation of the available data suggests that IHABP is a Bach1-anchoring protein. Third, FRAP analysis revealed the dynamic nature of the Bach1-IHABP interaction in a living cell. This finding excludes the possibility that the Bach1-IHABP complex reflects non-functional protein aggregation due to overexpression. Rather, the dynamic interaction strongly supports that IHABP shifts the equilibrium of Bach1 distribution. Because Bach1 is regulated by nuclear export, the presence of IHABP in the cytoplasmic region is likely to facilitate cytoplasmic accumulation.

The subcellular localization of transcription factors is often regulated by association with cytoskeletal proteins. For example, the direct association between the SAMD protein and microtubules negatively regulates TGF-β signalling (*29*). A direct association between the myc-interacting zinc finger protein (MIZ-1) and microtubules is involved in the transcriptional regulation of the low-density lipoprotein receptor (LDLR) gene (*30*). An association between the Cubitus interruptus(Ci) transcription factor and microtubule-binding protein, Costal-2, is critically important in the Drosophila hedgehog pathway (*31*). An actin-binding protein, Keap1, interacts with Nrf2, sequestering it in the cytoplasmic region (*32*, *33*) . However, the dynamics of such interactions in living cells remains to be explored. We found here that the interaction between Bach1 and IHABP is in dynamic equilibrium. This observation suggests that slight changes in the amounts of proteins or binding affinity, which may be achieved by protein modification, can substantially affect the nuclear amount of Bach1. Taken together with our previous findings, we suggest the integrated model depicted in Fig. 8. In this model, the subcellular distribution of Bach1 is determined by three factors: constitutive nuclear import, cadmium- and heme-inducible nuclear export, and cytoskeletal anchoring by IHABP. Distinct nuclear export signals on Bach1 are involved in the heme and cadmium responses. Once exported from nuclei, IHABP anchors Bach1 in a dynamic way in the cytoplasmic region, allowing the induction of Bach1 target genes such as HO-1 by Nrf2 (*34*, *35*) or other activators. When oxidative stress is reduced or heme levels are lowered due to HO-1 activity, the nuclear export of Bach1 is inactivated. Because of the dynamic nature of the anchoring by IHABP, Bach1 would now readily accumulate within the nuclei to reassume repression. Such a combination of dynamic regulations of Bach1 activity appears important to achieve the conditional expression of target genes such as HO-1 in response to various physiological and pathological stimuli.

The fact that IHABP is a microtubule-associated protein raises important questions in terms of Bach1 regulation. First, because cytoskeletal structures change during the cell cycle, one may wonder whether the Bach1-IHABP interaction is also under cell cycle control. Second, because cytoskeletal structures change in response to various stresses (*36–41*), the inducible expression of HO-1 may also be achieved, at least in part, through changes in cytoskeletal structures. Further studies along these lines may shed light on how Bach1 regulates gene expression in the context of the cell cycle and stress responses.

We thank Ms. Maria Makri, Imperial College of London, for comments on the manuscript and Dr. Volker Assmann, King's College London, for the IHABP cDNA clones. This work was

supported by Grants-in-aid from the Ministry of Education, Science, Sport and Culture of Japan.

REFERENCES

1. Otterbein, L.E., Soares, M.P., Yamashita, K., and Bach, F.H. (2003) Heme oxygenase-1: unleashing the protective properties of heme. *Trends Immunol.* **24**, 449–455
2. Alam, J., Shibahara, S., and Smith, A. (1989) Transcriptional activation of the heme oxygenase gene by heme and cadmium in mouse hepatoma cells. *J. Biol. Chem.* **264**, 6371–6375
3. Shibahara, S. (2003) The heme oxygenase dilemma in cellular homeostasis: new insights for the feedback regulation of heme catabolism. *Tohoku J. Exp. Med.* **200**, 167–186
4. Ryter, S.W., Otterbein, L.E., Morse, D., and Choi, A.M. (2002) Heme oxygenase/carbon monoxide signaling pathways: regulation and functional significance. *Mol. Cell. Biochem.* 234–235, 249–263
5. Katori, M., Anselmo, D.M., Busuttil, R.W., and Kupiec-Weglinski, J.W. (2002) A novel strategy against ischemia and reperfusion injury: cytoprotection with heme oxygenase system. *Transpl. Immunol.* **9**, 227–233
6. Yachie, A., Niida, Y., Wada, T., Igarashi, N., Kaneda, H., Toma, T., Ohta, K., Kasahara, Y., and Koizumi, S. (1999) Oxidative stress causes enhanced endothelial cell injury in human heme oxygenase-1 deficiency. *J. Clin. Invest.* **103**, 129–135
7. Poss, K.D., and Tonegawa, S. (1997) Reduced stress defense in heme oxygenase 1-deficient cells. *Proc. Natl Acad. Sci. USA* **94**, 10925–10930
8. Inamdar, N.M., Ahn, Y.I., and Alam, J. (1996) The heme-responsive element of the mouse heme oxygenase-1 gene is an extended AP-1 binding site that resembles the recognition sequences for MAF and NF-E2 transcription factors. *Biochem. Biophys. Res. Commun.* **221**, 570–576
9. Kataoka, K., Noda, M., and Nishizawa, M. (1994) Maf nuclear oncoprotein recognizes sequences related to an AP-1 site and forms heterodimers with both Fos and Jun. *Mol. Cell. Biol.* **14**, 700–712
10. Itoh, K., Chiba, T., Takahashi, S., Ishii, T., Igarashi, K., Katoh, Y., Oyake, T., Hayashi, N., Satoh, K., Hatayama, I., Yamamoto, M., and Nabeshima, Y. (1997) An Nrf2/small Maf heterodimer mediates the induction of phase II detoxifying enzyme genes through antioxidant response elements. *Biochem. Biophys. Res. Commun.* **236**, 313–322
11. Ishii, T., Itoh, K., Takahashi, S., Sato, H., Yanagawa, T., Katoh, Y., Bannai, S., and Yamamoto, M. (2000) Transcription factor Nrf2 coordinately regulates a group of oxidative stress-inducible genes in macrophages. *J. Biol. Chem.* **275**, 16023–16029
12. Alam, J., Wicks, C., Stewart, D., Gong, P., Touchard, C., Otterbein, S., Choi, A.M., Burow, M.E., and Tou, J. (2000) Mechanism of heme oxygenase-1 gene activation by cadmium in MCF-7 mammary epithelial cells. Role of p38 kinase and Nrf2 transcription factor. *J. Biol. Chem.* **275**, 27694–27702
13. Kataoka, K., Handa, H., and Nishizawa, M. (2001) Induction of cellular antioxidative stress genes through heterodimeric transcription factor Nrf2/small Maf by antirheumatic gold(I) compounds. *J. Biol. Chem.* **276**, 34074–34081
14. Sun, J., Hoshino, H., Takaku, K., Nakajima, O., Muto, A., Suzuki, H., Tashiro, S., Takahashi, S., Shibahara, S., Alam, J., Taketo, M.M., Yamamoto, M., and Igarashi, K. (2002) Hemoprotein Bach1 regulates enhancer availability of heme oxygenase-1 gene. *EMBO J.* **21**, 5216–5224
15. Sun, J., Brand, M., Zenke, Y., Tashiro, S., Groudine, M., and Igarashi, K. (2004) Heme regulates the dynamic exchange of Bach1 and NF-E2-related factors in the Maf transcription factor network. *Proc. Natl Acad. Sci. USA* **101**, 1461–1466
16. Suzuki, H., Tashiro, S., Sun, J., Doi, H., Satomi, S., and Igarashi, K. (2003) Cadmium induces nuclear export of Bach1, a transcriptional repressor of heme oxygenase-1 gene. *J. Biol. Chem.* **278**, 49246–49253
17. Suzuki, H., Tashiro, S., Hira, S., Sun, J., Yamazaki, C., Zenke, Y., Ikeda-Saito, M., Yoshida, M., and Igarashi, K. (2004) Heme regulates gene expression by triggering Crm1-dependent nuclear export of Bach1. *EMBO J.* **23**, 2544–2553
18. Maxwell, C.A., Keats, J.J., Crainie, M., Sun, X., Yen, T., Shibuya, E., Hendzel, M., Chan, G., and Pilarski, L.M. (2003) RHAMM is a centrosomal protein that interacts with dynein and maintains spindle pole stability. *Mol. Biol. Cell* **14**, 2262–2276
19. Assmann, V., Marshall, J.F., Fieber, C., Hofmann, M., and Hart, I.R. (1998) The human hyaluronan receptor RHAMM is expressed as an intracellular protein in breast cancer cells. *J. Cell Sci.* **111** (Pt 12), 1685–1694
20. Assmann, V., Jenkinson, D., Marshall, J.F., and Hart, I.R. (1999) The intracellular hyaluronan receptor RHAMM/IHABP interacts with microtubules and actin filaments. *J. Cell Sci.* **112** (Pt 22), 3943–3954
21. Assmann, V., Gillett, C.E., Poulsom, R., Ryder, K., Hart, I.R., and Hanby, A.M. (2001) The pattern of expression of the microtubule-binding protein RHAMM/IHABP in mammary carcinoma suggests a role in the invasive behaviour of tumour cells. *J. Pathol.* **195**, 191–196
22. Hofmann, M., Fieber, C., Assmann, V., Gottlicher, M., Sleeman, J., Plug, R., Howells, N., von Stein, O., Ponta, H., and Herrlich, P. (1998) Identification of IHABP, a 95 kDa intracellular hyaluronate binding protein. *J. Cell Sci.* **111** (Pt 12), 1673–1684
23. Oyake, T., Itoh, K., Motohashi, H., Hayashi, N., Hoshino, H., Nishizawa, M., Yamamoto, M., and Igarashi, K. (1996) Bach proteins belong to a novel family of BTB-basic leucine zipper transcription factors that interact with MafK and regulate transcription through the NF-E2 site. *Mol. Cell. Biol.* **16**, 6083–6095
24. Tashiro, S., Muto, A., Tanimoto, K., Tsuchiya, H., Suzuki, H., Hoshino, H., Yoshida, M., Walter, J., and Igarashi, K. (2004) Repression of PML nuclear body-associated transcription by oxidative stress-activated Bach2. *Mol. Cell. Biol.* **24**, 3473–3484
25. Muto, A., Hoshino, H., Madisen, L., Yanai, N., Obinata, M., Karasuyama, H., Hayashi, N., Nakauchi, H., Yamamoto, M., Groudine, M., and Igarashi, K. (1998) Identification of Bach2 as a B-cell-specific partner for small maf proteins that negatively regulate the immunoglobulin heavy chain gene 3′ enhancer. *EMBO J.* **17**, 5734–5743
26. Phair, R.D., Scaffidi, P., Elbi, C., Vecerova, J., Dey, A., Ozato, K., Brown, D.T., Hager, G., Bustin, M., and Misteli, T. (2004) Global nature of dynamic protein-chromatin interactions *in vivo*: three-dimensional genome scanning and dynamic interaction networks of chromatin proteins. *Mol. Cell. Biol.* **24**, 6393–6402
27. Gundersen, G.G. and Cook, T.A. (1999) Microtubules and signal transduction. *Curr. Opin. Cell Biol.* **11**, 81–94
28. Lynn, B.D., Li, X., Cattini, P.A., and Nagy, J.I. (2001) Sequence, protein expression and extracellular-regulated kinase association of the hyaladherin RHAMM (receptor for hyaluronan mediated motility) in PC12 cells. *Neurosci. Lett.* **306**, 49–52
29. Dong, C., Li, Z., Alvarez, R., Jr., Feng, X.H., and Goldschmidt-Clermont, P.J. (2000) Microtubule binding to Smads may regulate TGF beta activity. *Mol. Cell* **5**, 27–34
30. Ziegelbauer, J., Shan, B., Yager, D., Larabell, C., Hoffmann, B., and Tjian, R. (2001) Transcription factor MIZ-1 is regulated *via* microtubule association. *Mol. Cell* **8**, 339–349
31. Ohlmeyer, J.T., and Kalderon, D. (1998) Hedgehog stimulates maturation of Cubitus interruptus into a labile transcriptional activator. *Nature* **396**, 749–753
32. Itoh, K., Wakabayashi, N., Katoh, Y., Ishii, T., Igarashi, K., Engel, J.D., and Yamamoto, M. (1999) Keap1 represses nuclear activation of antioxidant responsive elements by Nrf2 through binding to the amino-terminal Neh2 domain. *Genes Dev.* **13**, 76–86
33. Itoh, K., Ishii, T., Wakabayashi, N., and Yamamoto, M. (1999) Regulatory mechanisms of cellular response to oxidative stress. *Free Radic. Res.* **31**, 319–324

34. Kang, K.W., Lee, S.J., Park, J.W., and Kim, S.G. (2002) Phosphatidylinositol 3-kinase regulates nuclear translocation of NF-E2-related factor 2 through actin rearrangement in response to oxidative stress. *Mol. Pharmacol.* **62**, 1001–1010
35. Alam, J., Stewart, D., Touchard, C., Boinapally, S., Choi, A.M., and Cook, J.L. (1999) Nrf2, a Cap'n'Collar transcription factor, regulates induction of the heme oxygenase-1 gene. *J. Biol. Chem.* **274**, 26071–26078
36. Liang, P. and MacRae, T.H. (1997) Molecular chaperones and the cytoskeleton. *J. Cell Sci.* **110** (Pt 13), 1431–1440
37. Lange, B.M. (2002) Integration of the centrosome in cell cycle control, stress response and signal transduction pathways. *Curr. Opin. Cell Biol.* **14**, 35–43
38. Debec, A. and Marcaillou, C. (1997) Structural alterations of the mitotic apparatus induced by the heat shock response in Drosophila cells. *Biol. Cell* **89**, 67–78
39. Sibon, O.C., Kelkar, A., Lemstra, W., and Theurkauf, W.E. (2000) DNA-replication/DNA-damage-dependent centrosome inactivation in Drosophila embryos. *Nat. Cell Biol.* **2**, 90–95
40. Pearce, A.K. and Humphrey, T.C. (2001) Integrating stress-response and cell-cycle checkpoint pathways. *Trends Cell Biol.* **11**, 426–433
41. Meraldi, P. and Nigg, E.A. (2002) The centrosome cycle. *FEBS Lett.* **521**, 9–13